Two-dimensional microscanner for laser projection

Yaobo Liu (刘耀波)*, **Weizheng Yuan (苑伟政)**, **Dayong Qiao (乔大勇)**,
Longfei Shi (史龙飞), and **Xiangnan Guo (郭向楠)**

Key Laboratory of Micro/Nano Systems for Aerospace, Ministry of Education, Xi'an 710072, China

**Corresponding author:liuyaobo2000@163.com*

Received November 19, 2012; accepted February 25, 2013; posted online May 30, 2013

The design of a two-dimensional (2D) microscanner actuated electrostatically is presented, and a silicon-on-insulator (SOI) micromachining process is utilized to fabricate the sample. The microscanner can oscillate at inherent frequencies of 1146 and 360 Hz around two rotational axes, generating maximum twisting angles of $\pm 10°$ and $\pm 5.3°$ under two 10-V square waves, respectively. A monochromatic laser projection system based on Lissajous pattern is demonstrated using the developed microscanner, revealing an image resolution of 168×56 at 20 frames per second.

OCIS codes: 230.0230, 110.0110, 330.0330.

doi: 10.3788/COL201311.062301.

With the adoption of microelectromechanical system technology, microscanners, as significant optical elements, are advantageous over conventional scanners because of their small size, light weight, low cost, and low power consumption. These characteristics make the microscanners suitable for application in optical fiber communication[1,2], biological imaging and tomography[3−5], barcode[6], and laser projection[7,8]. Microscanners can greatly improve the compactness and portability of so-developed projectors, enabling the integration of such devices into mobile phones, notebook computers, and other portable electronic equipments. Hence, laser projection based on microscanners has been a research focus in recent years.

Depending on the different driving mechanisms, several methods are used to actuate microscanners, which can be mainly classified as magnetic, piezoelectric, electrostatic, and thermal actuators[9−14]. Thermal actuators reveal a comparatively slow response to the driving signal. Generally, magnetic actuators can offer a large driving force, which is a significant advantage of microscanners. However, the micromachining process is complex because of the deposited coils, and the volume after packaging is bulky because of the assembly of permanent magnets. Piezoelectric actuators can respond rapidly to driving signals, but the complicated fabrication of piezoelectric materials increases the difficulty in the development of these microscanners. Compared with magnetic and piezoelectric actuators, electrostatic actuators attract more interest because of their outstanding advantages in terms of simplicity of structure, compactness of volume, and simplicity of the micromachining process, although the driving force is relatively small.

In this letter, a two-dimensional (2D) electrostatically actuated microscanner is presented, and the sample is fabricated using a silicon-on-insulator (SOI) micromachining process. Then, the principle of laser projection based on Lissajous pattern is described, and the prototype of a monochrome laser projector is demonstrated by employing the achieved microscanner.

Figure 1 depicts the schematic diagram of the designed 2D microscanner, which consists of a mirror, a movable frame, and a fixed frame (Fig. 1(a)). Rectangular torsional beams were utilized to connect all the three parts. The enlarged picture in Fig. 1(b) illustrates the isolation trench employed to realize the electrical isolation between the mirror and movable frame. To actuate the microscanner, the initial vertical offset was purposely introduced between the interdigitated comb fingers of the mirror and the frame (Fig. 1(c)), which was only used as the starting electrode and was nonsignificant to the characterization of the microscanner. The bottom of the whole device was removed to allow enough space for structural deflection and avoid the adhesion problem during the release of movable structures. Table 1 shows the main structural parameters of the microscanner.

A 2D microscanner is essentially equivalent to two one-dimensional (1D) microscanners, the driving principle of which is shown in Fig. 2. A square wave was used as the excitation signal, and the switch-off time of the driving signal coincided with the moment the mirror plates pass the resting position. The frequency of the driving signal is twice that of the mechanical oscillation. Additionally, a triangular wave, sawtooth wave, or sine wave can also be employed as the excitation signal for the microscanner. Compared with the square wave, however, the oscillation amplitude caused by all the other waves

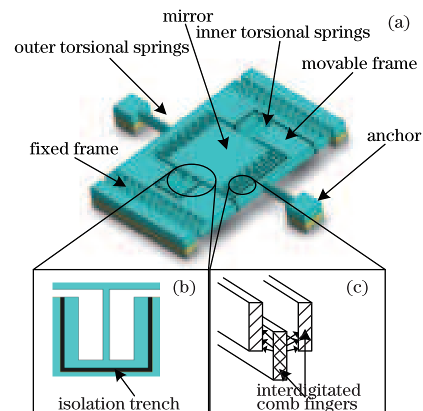

Fig. 1. Schematic diagram of the designed 2D microscanner. (a) Structure of the 2D microscanner; (b) enlarged picture of the isolation trench; (c) structure of the interdigitated comb fingers.

 © 2013 Chinese Optics Letters

mentioned slightly decrease at the same applied voltage.

Figure 3 demonstrates the flow chart of the SOI micromachining process for fabricating the microscanner. A SOI wafer (100), with a 30-μm-thick device layer, 1-μm buried oxide (BOX) layer, and 400-μm handle layer, was used as the starting material.

The process began with etching of the trench in the device layer by lithography and inductively coupled plasma (ICP) etching (Fig. 3(a)). Next, a 100-nm-thick oxide film was grown by wet oxidation, and the trench was filled with polysilicon by low pressure chemical vapor deposition (Fig. 3(b)). The polysilicon over the wafer was then removed by chemical-mechanical polishing before depositing an aluminum film over the handle layer. Then, the aluminum film was patterned by wet etching (Fig. 3(c)). To ensure the mirror's movement, the silicon underneath the moving parts was removed by ICP etching, and the structures, including the inner mirror, combs, and outer frame, were made using the same micromachining process as shown in Fig. 3(a). Finally, the structures were released with hydrofluoric acid (HF)

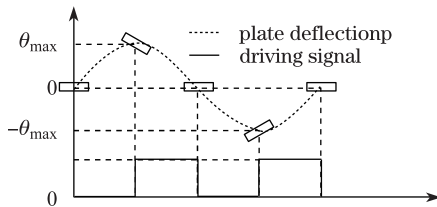

Fig. 2. Driving principle of the 1D microscanner.

Table 1. Main Structural Parameters of Microscanner.

Structural Parameter	Value (μm)
Mirror Plate	1 500×1 500
Inner Torsional Springs	
Length	400
Width	10
Outer Torsional Springs	
Length	300
Width	10
Outer Frame	
Length	2 900
Width	2 300

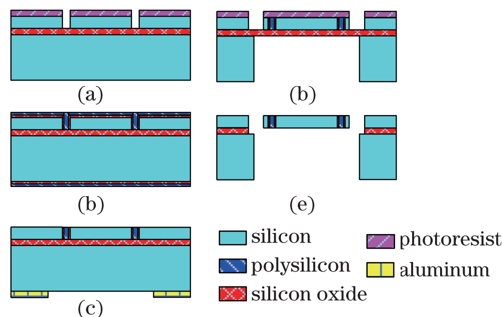

Fig. 3. (Color online) Flow chart of the SOI micromachining process for fabricating the microscanner.

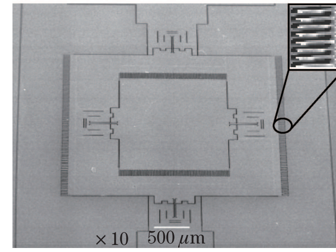

Fig. 4. Scanning electron micrograph of the fabricated microscanner.

etching to remove the BOX layer below all the movable components (Fig. 3(e)).

Ideally, all the combs should be of the same altitude, because they are fabricated on the same device layer. Therefore, no vertical offset should exist between the fixed and movable fingers. However, avoiding the residual stress generated during the fabrication is difficult and causes mechanical deformation of the fabricated structures. As a result, a slightly vertical comb offset will appear ultimately. Figure 4 shows a scanning electron micrograph of the fabricated microscanner, and the vertical comb offset can be observed clearly in the inset. Figure 5 shows a picture of the microscanner chip after wire bonding and packaging.

Figure 6 demonstrates the frequency response of the microscanner when the driving voltages are two 10-V square waves, which is an essential characteristic of a microscanner. Clearly, the resonance curve shows a significant hysteresis because the microscanner is a typical parametrically excited system. However, the microscanner can only oscillate at the inherent frequencies of 1 146 and 360 Hz around the two rotational axes if the excitation frequency is swept down from a higher initial value, generating maximum twisting angles of $\pm10°$ and $\pm5.3°$, respectively. In addition, the maximum and minimum driving voltages for the sample actuation are tested to be 42 and 5 V, respectively. Thus, the sample has easier micromachining process and higher drive efficiency compared with the microscanner reported in the reference.

Considering that the mirror demonstrates a sinusoidal rotating movement around both the x- and y-axes when the microscanner is operated, the trajectory of the laser beam deflected by the microscanner exhibits the Lissajous pattern[15]. Figure 7 shows the schematic diagram of the laser projection using a 2D microscanner. Significantly, selecting the appropriate oscillation frequencies around the x- and y-axes is crucial for projection and is important for determining the density and period of the Lissajous pattern.

As shown in Fig. 7, every pixel can be theoretically represented by a section of one scanning line within the corresponding grid because the Lissajous pattern is stable and invariable, and the number of grids could be used to evaluate the resolution if the scanning line gets through each grid at least once. Obviously, the greater the density is, the higher the resolution will be. Consequently, every pixel can be projected by accurately switching on the laser at the corresponding moment, and the gray information can be realized by adjusting the laser driving current.

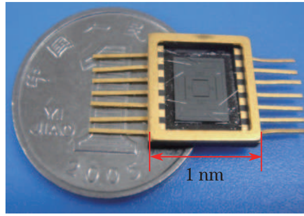

Fig. 5. Picture of the microscanner chip after wire bonding and packaging.

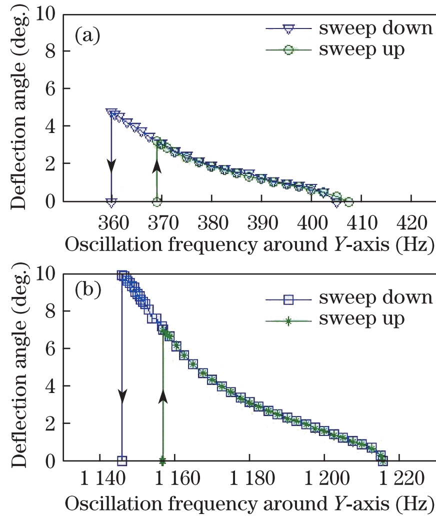

Fig. 6. (Color online) Mirror rotation angle versus oscillation frequency.

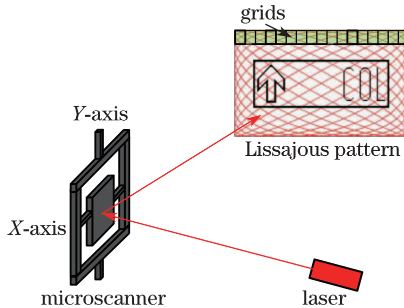

Fig. 7. Schematic diagram of laser projection using a 2D microscanner.

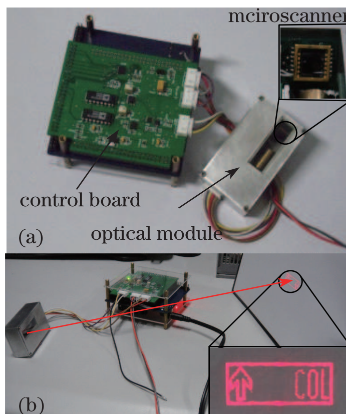

Fig. 8. Prototype of a monochrome laser projector. (a) The built projection equipment and (b) actual projection effect.

Figure 8 shows the prototype of a monochrome laser projector which has been successfully built. As shown in Fig. 8(a), the prototype is composed of the controlling board and the optical module. The controlling board is utilized to dominate the on-off time and driving current for laser according to the information of the projecting image. The practical result is shown in Fig. 8(b). The resolution is 168×56, and the refresh rate is 20 frames per second. The oscillation frequencies around the x- and $y-$axes are 1160 and 380 Hz, respectively. Evidently, the experimental result provides exactly what we want to project.

In conclusion, an electrostatically driven 2D microscanner based on the SOI technology is designed and fabricated. Given the sinusoidal movement of the inner mirror both in the x and y directions, the microscanner can be used for laser projection based on the Lissajous pattern and the prototype of a monochrome laser projector, which has been successfully built using the achieved microscanner. The resolution and the refresh rate are 168×56 and 20 frames per second, respectively, and the two oscillation frequencies are 1160 and 380 Hz. Further work should be aimed at improving the resolution and the refresh rate of the projector and at realizing full-color projection.

This work was supported by the Program for the New Century Excellent Talents in University, Ministry of Education of China (No. NCET-10-0075) and the National Natural Science Foundation of China (No. 50805123).

References

1. J. Tsai, S. Huang, D. Hah, and M. C. Wu, J. Lightwave Technol. **24,** 897 (2006).
2. D. T. Neilson, R. Frahm, P. Kolodner, C. A. Bolle, R. Ryf, J. Kim, A. R. Papazian, C. J. Nuzman, A. Gasparyan, N. R. Basavanhally, V. A. Aksyuk, and J. V. Gates, J. Lightwave Technol. **22,** 1499 (2004).
3. C. Chong, K. Isamoto, and H. Toshiyoshi, IEEE Photon. Technol. Lett. **18,** 133 (2006).
4. A. D. Aguirre, P. R. Herz, Y. Chen, J. G. Fujimoto, W. Piyawattanametha, L. Fan, and M. C. Wu, Opt. Express. **15,** 2445 (2007).
5. T. Xie, H. Xie, G. K. Fedder, and Y. Pan, Appl. Opt. **42,** 6422 (2003).
6. A. D. Yalcinkaya, O. Ergeneman, and H. Urey, Sens. Actuators A Phys. **135,** 236 (2007).
7. A. D. Yalcinkaya, H. Urey, D. Brown, T. Montague, and R. Sprague, J. Microelectromech. Syst. **15,** 786 (2006).
8. Y. C. Ko, J. W. Cho, Y. K. Mun, H. G. Jeong, W. K. Choi, J. H. Lee, J. W. Kim, J. B. Yoo, and J. H. Lee, Sens. Actuators A Phys. **126,** 218 (2006).
9. K. H. Koh and C. Lee, J. Microelectromech. Syst. **21,** 1124(2012).
10. H. Schenk, P. Dürr, T. Haase, D. Kunze, U. Sobe, H. Lakner, and H. Zück, IEEE J. Select. Top. Quant. Electron. **6,** 715 (2000).
11. C. Lee, Sens. Actuators A Phys. **115,** 581(2004).
12. W. Piyawattanametha, P. R. Patterson, D. Hah, H. Toshiyoshi, and M. C. Wu, J. Microelectromech. Syst. **14,** 1329 (2005).
13. C. H. Ji, M. Choi, S. C. Kim, K. C. Song, J. U. Bu, and H. J. Nam, J. Microelectromech. Syst. **16,** 989 (2007).
14. K. H. Koh, T. Kobayashi, and C. Lee, Opt. Express **19,** 13812 (2011).
15. M. Scholles, A. Bräuer, K. Frommhagena, C. Gerwiga, H. Lakner, H. Schenka, and M. Schwarzenberga, Proc. SPIE **6466,** 64660A (2007).